Journal of Materials and Environmental Sciences
ISSN : 2028-2508

JMES, 2017 Volume 8, Issue 9, Page 3303-3312

http://www.jmaterenvironsci.com/

The effect of Antimony (Sb) additive on the kinetics of glass transition and crystallization of SeM (M=In, Zn) chalcogenide glasses

M. M. Heireche[1, 2, *], K. Driss Khodja[2], L. Heireche[3], N. E. Benaioun[2], B. Amrani[2]

[1] *Département des sciences exactes, Ecole Normale Supérieure (ENS) d'Oran.*
[2] *Laboratoire de Physique des Couches Minces et Matériaux pour l'Electronique (LPC2ME), Université d'Oran1, Oran, Algeria.*
[3] *Laboratoire des Sciences de la Matière Condensée, Université d'Oran1, Oran, Algeria.*

Received 12 Oct 2016,
Revised 08 Dec 2016,
Accepted 14 Dec 2016

Keywords

- ✓ Glass transition,
- ✓ Chalcogenide Glasses,
- ✓ Crystallization temperature,
- ✓ Activation energy,
- ✓ Differential scanning calorimetry

heirechemohamed@yahoo.fr
+213672419895

Abstract

In the present work we study the effect of addition of Antimony Sb content on various thermal parameters in binary SeIn and SeZn glassy systems. The crystallization and glass transition kinetics of $Se_{90-x}M_{10}Sb_x$ (M= In, Zn) chalcogenide glasses were studied under non-isothermal condition using a Differential Scanning Calorimeter (DSC). The activation energy of glass transition E_g, Avrami index n, dimensionality of growth m and activation energy of crystallization E_c have been determined from different models. Thermal stability has also been determined from the temperature difference between the onset crystallization and glass transition temperature.

Introduction

Chalcogenide materials are becoming more and more popular due to their applications as infrared optical fibers [1], reversible phase change optical recording [2], memory switching [3], X-ray imaging [4], xerography [5], electrographic applications such as photoreceptors in photocopying and laser printing [6-8]. A lot of work has-been done on optical, electrical and thermal properties of chalcogenide glasses [9-20]. The binary Se-In alloys have more advantages due to their greater hardness, higher crystallisation temperature, higher photosensitivity and smaller ageing effects [21]. The energy band of glassy Se-In alloys is about 1.3 at 300K [22].

The binary Se-Zn alloys have more advantages due to their wide band gap, they are an example of potential applications in optoelectronic devices like blue light emitting diodes and blue diode lasers [21] and white Light Emitting Diodes (LEDs) and infrared lenses [23].

The addition of third element in the SeM (M=In, Zn) glasses converts the glasses into an interesting material and compound has a special effect on structural, optical, electronic and thermal properties. With this point of view Sb has been added to SeM (M=In, Zn), which will create the compositional and configurational disorder in the material as compared to binary alloy. The present work is concerned with the study of the effect of Sb incorporation on various thermal parameters in binary SeIn and SeZn glassy systems. We have therefore used non-isothermal measurements (DSC technique) for study the glass transition and crystallization kinetics in SeMSb (M=In, Zn) glassy systems. The activation energy associated with the glass-transition E_g, the activation energy of crystallization E_c are calculated at different compositions by using different kinetics models. The dependence of glass transition temperature on heating rate was rationalized and correlated using Lasocka equation and the Avrami exponent also has been determined to study nucleation and growth during crystallization process.

2. Experimental

Bulk sample of the $Se_{90-x}M_{10}Sb_x$ (M= In, Zn) x= (0, 2, 4) were prepared by the melt quenching technique, high purity (99.999%) elements were weighed according to their atomic percentage, and were sealed in a quartz ampoule in a vacuum (10^{-5}torr).

The sealed ampoules were placed inside a furnace and the temperature of the furnace was raised from room temperature to 800°C at a rate of 4°C/min, the ampoules were rocked frequently for 10h to make the melt homogeneous, each ampoule is then quenched in icy water to obtain the composition in the glass state.

The glassy nature was confirmed by using X-ray diffraction technique which shown in Figure 1.

For DSC studies, we have taken 10 mg of each sample of $Se_{90-x}M_{10}Sb_x$ (M= In, Zn) glassy alloys. The DSC scans were taken at different heating rates 5, 7, 10, and 12 °C/min.

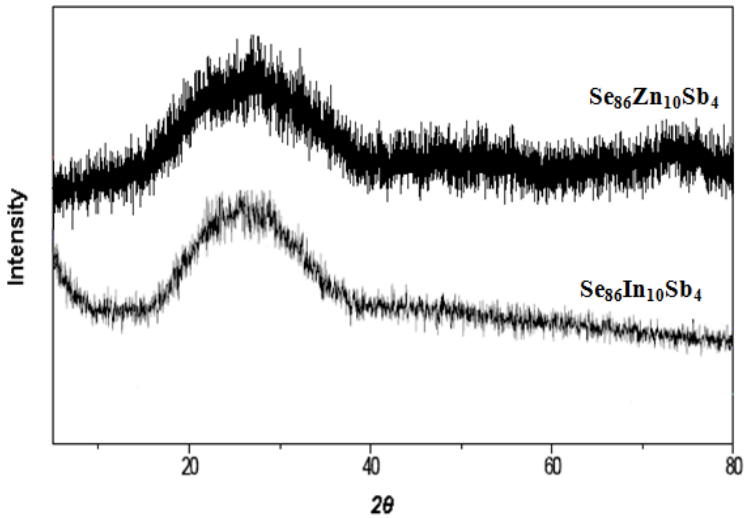

Figure 1: XRD pattern of $Se_{86}In_{10}Sb_4$ and $Se_{86}Zn_{10}Sb_4$ glasses

3. Results and discussion

Figure 2 shows typical DSC thermograms for glassy $Se_{88}In_{10}Sb_2$ and $Se_{88}Zn_{10}Sb_2$ at heating rate 10 K/min, similar thermograms were obtained for other heating rates also (not shown here). The single endothermic and exothermic peaks are observed at the glass-transition temperature T_g and the crystallization temperature T_c respectively.

The first endothermic peak correspond to the glass transition, the second exothermic peak indicate the crystallisation of $Se_{90-x}M_{10}Sb_x$ (M= In, Zn) and the endothermic peak present the melting of sample. The obtained values of glass transition temperature T_g and crystallization temperature T_c with different compositions and heating rates at 5, 7, 10 and 12 K/min are given in Table 1.

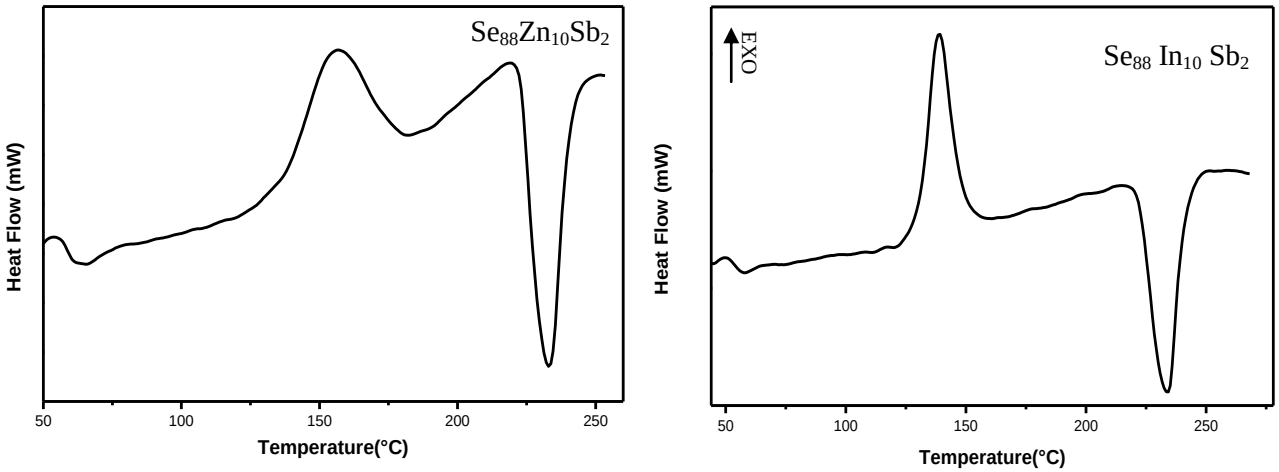

Figure 2: DSC thermograms of $Se_{88}In_{10}Sb_2$ and $Se_{88}Zn_{10}Sb_2$ glassy alloys at heating rate of 10°C/min

Table 1: The values of glass transition temperature T_g and crystallization temperature T_c at different heating rates 5, 7, 10, 12°C/min for $Se_{90-x}In_{10}Sb_x$ and $Se_{90-x}Zn_{10}Sb_x$ (x=0, 2, 4) glassy alloys.

	X=In						X=Zn					
Heating rate	$Se_{90}In_{10}$		$Se_{88}In_{10}Sb_2$		$Se_{86}In_{10}Sb_4$		$Se_{90}Zn_{10}$		$Se_{88}Zn_{10}Sb_2$		$Se_{86}Zn_{10}Sb_4$	
(°C/min)	T_g / K	T_c /K	T_g / K	T_c / K	T_g / K	T_c / K	T_g (K)	T_c(K)	T_g(K)	T_c(K)	T_g(K)	T_c(K)
05	319	394	325	389	327	388	325	374	323	388	321	3**91**
07	323	398	328	396	329	395	328	377	326	397	325	403
10	326	405	330	401	330	400	331	381	329	401	327	408
12	328	407	331	404	333	402	332	385	331	405	328	412

3.1. Glass transition region

From Table 1, it is clear that T_g and T_c both shift towards higher temperatures as the heating rate increases from 7 to 12C°/min. The dependence of T_g on the heating rate is investigated using two approaches. The first is through an empirical relationship introduced by Lasocka [24].

$$T_g = A + B\ln\alpha \qquad (1)$$

where A and B are constants for a given glass composition, the value of A indicates the glass transition temperature for the heating rate of 1 K /min, while B is proportional to the time taken by the system to reduce its glass transition temperature (T_g) , when its heating rate is lowered from 10 to 1 K/min [25].
Figure 3 depicts the variation of the glass transition temperature T_g with lnα for the investigated $Se_{90-x}In_{10}Sb_x$ (x=0, 2, 4) and $Se_{90-x}Zn_{10}Sb_x$ (x=0, 2, 4) glassy systems. From figure 4.5 the values of A and B can be obtained form the slop of straight line of the plot T_g versus lnα
The calculated values of A and B for the different compositions are listed in Table 2.

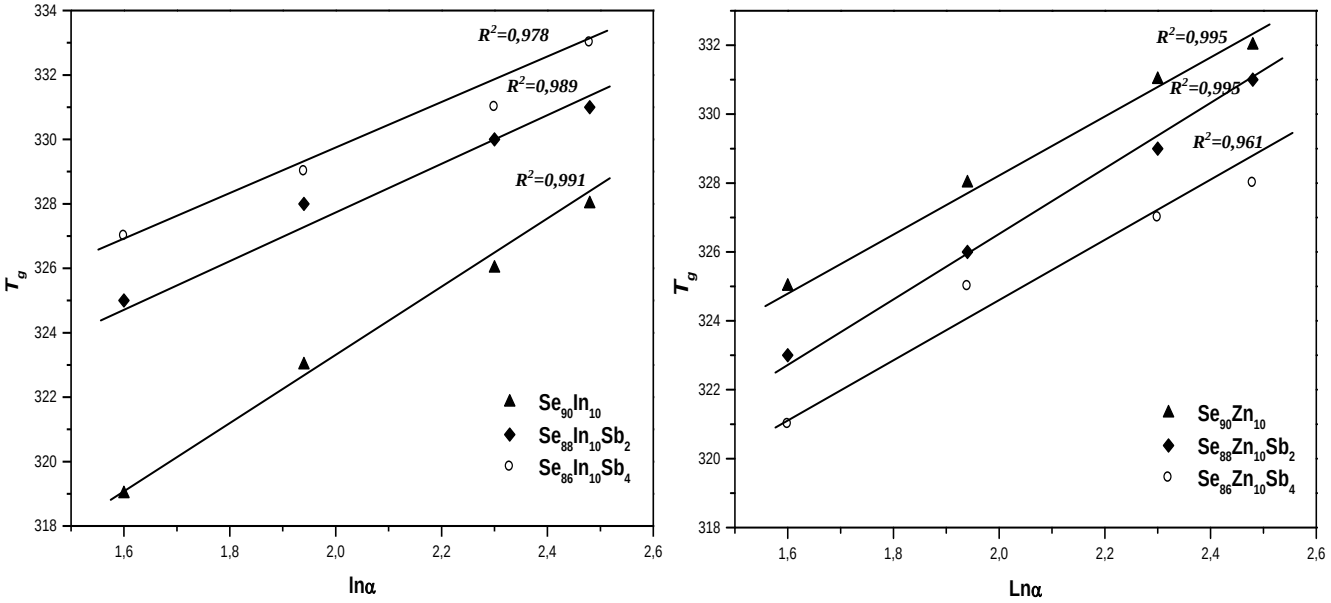

Fig. 3: Plots of T_g versus lnα along with linear fits for $Se_{90-x}Zn_{10}Sb_x$ (x = 0, 2, 4) and $Se_{90-x}In_{10}Sb_x$ (x = 0, 2, 4) glasses.

It is clear from Table 2 that the values of the constant B are dependent on the compositions, which indicates the change in the structure with additive Sb content.

The second approach is the evaluation of the activation energy for the glass transition (Eg) using Kissingers formula [26]

$$\ln\left(\alpha / T_{gp}^{\,2}\right) = -E_g / RT_{gp} + \text{constant} \qquad (2)$$

Where E_g is the activation energy of the glass transition, T_{gp} is the peak glass transition temperature, α is the heating rate and R is the universal gas constant.

In Figure 4, $\ln(\alpha / T_{gp}^{\,2})$ has been plotted against $1000/T_{gp}$ for the different compositions $Se_{90-x}In_{10}Sb_x$ (x = 0, 2, 4) and $Se_{90-x}Zn_{10}Sb_x$ (x=0, 2, 4) . The values of E_g were evaluated and are listed in Table 2. It is observed that the glass transition activation energy decreases with increasing Sb content, this variation of E_g can be explained on the basses of structural changes due to the introduction of Sb.

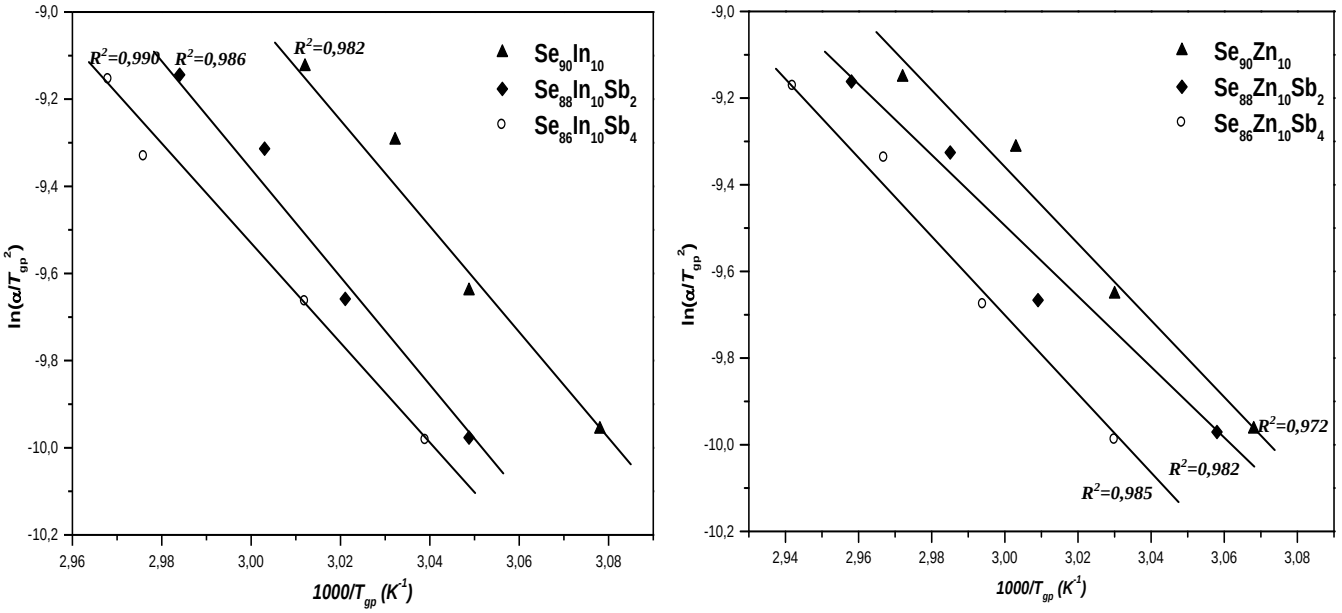

Figure 4: Linear *fit* of the Kissinger plots for determining E_g associated with the glass transition peaks for $Se_{90-x}In_{10}Sb_x$ (x=0, 2, 4) and $Se_{90-x}Zn_{10}Sb_x$ (x = 0, 2, 4) glasses.

Table 2: The values of *A*, *B* and Activation energy of glass transition E_g for $Se_{90-x}In_{10}Sb_x$ and $Se_{90-x}Zn_{10}Sb_x$ (x=0, 2, 4) glassy alloys.

Composition	*A* / K	*B* / min	E_g / KJ.mol^{-1}
$Se_{90}In_{10}$	303.03 ± 1.09	10.05 ± 0.51	130.00 ± 8.97
$Se_{88}In_{10}Sb_2$	314.40 ± 1.25	6.77 ± 0.60	102.48 ± 9.14
$Se_{86}In_{10}Sb_4$	316.00 ± 1.30	6.58 ± 0.61	93.50 ± 5.98
$Se_{90}Zn_{10}$	312.30 ± 0.79	8.01 ± 0.37	73.92 ± 0.85
$Se_{88}Zn_{10}Sb_2$	308.84 ± 1.67	9.02 ± 0.79	70.65 ± 1.03
$Se_{86}Zn_{10}Sb_4$	307.33 ± 1.90	8.70 ± 0.90	68.98 ± 0.74

3.2. Crystallization region

The crystallization fraction *x*, can be expressed as a function of time according to the Johnson–Mehl–Avrami equation [27-29] :

$$x(t) = 1 - \exp\left[-(kt)^n\right] \qquad (3)$$

Where n is the Avrami exponent which depends on the mechanism of growth and dimensionality of the crystal growth and K is defined as the reaction rate constant and is given by:

$$K = K_0 \exp\left(-E_c/kT\right) \qquad (4)$$

Where E_c is the activation on energy of crystallization, k is the Boltzmann constant, T is the isothermal temperature and K_0 is the frequency factor. The activation energy of crystallization E_c for $Se_{90-x}M_{10}Sb_x$ (M= In, Zn) glassy system have been determined using Matusita, Kissinger and Ozawa methods

3.2.1Matisita method

In the non-isothermal method, the crystallized fraction in a glass heated at a constant rate a is related to the activation energy of crystallization (Ec) is given by Matusita's [30,31] relation

$$\ln\left[-\ln(1-x)\right] = -n\ln\alpha - 1.052\,mE_c/RT + \text{constant} \qquad (5)$$

where x is the crystallized fraction and m and n are integer or half integer numbers that depend upon the growth mechanism and the dimensionality of the glassy alloy. Here $n = m + 1$ is taken for a quenched glass containing no nuclei and $n = m$ for a preheated glass containing sufficiently large number of nuclei, the values of n and m for different crystallization are given in Table 3. The fraction volume x crystallized at any temperature T is given as $x = S/S_T$, where S_T is the total area of the exotherm between T_i where the crystallization just begins and the temperature T_f *where* the crystallization is completed and S is the area between T_i and T.

Table 3: The Values of *n* and *m* for different crystallization mechanism

Mechanism	*n*	*m*
Three-dimensional growth	4	3
Two-dimensional growth	3	2
One-dimensional growth	2	1
Surface nucleation	1	1

Dimensionality of growth m and n values can be obtained from Matusita equation for each composition. The Avrami exponent n was calculated by plotting ln [-ln (1 - x)] versus lnα at specific temperatures. Figure 5 shows the variation of ln [-ln (1 - x)] versus lnα at three different temperatures for the composition $Se_{88}In_{10}Sb_2$ and $Se_{88}Zn_{10}Sb_2$. The deduced average values of n for different compositions is listed in Table 4.5

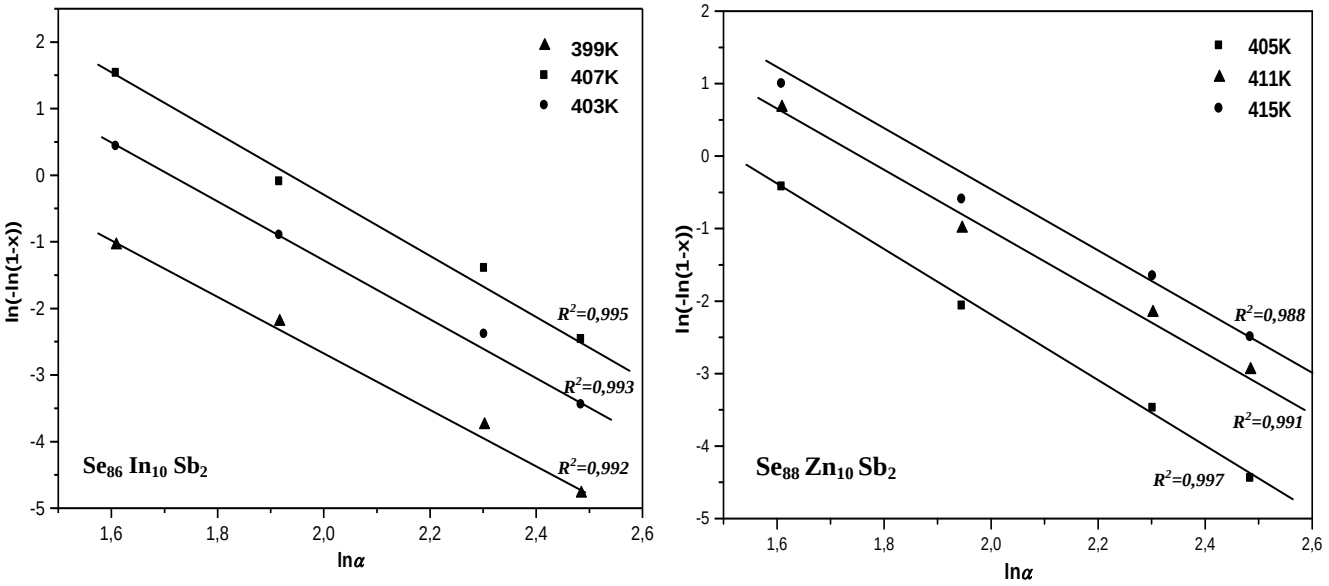

Figure 5: Linear fit of the Matusita plots for different composition $Se_{88}In_{10}Sb_2$ and $Se_{88}Zn_{10}Sb_2$ at three fixed temperature.

In general the values of n for different crystal mechanisms reveal the mechanism of crystal growth for different chalcogenide glasses (n = 4) for three-dimensional growth, n = 3 two-dimensional growth, n = 2 one-dimensional growth and n = 1 for surface nucleation [32, 33].
From Table 4, 5 it is observed that the values reveal the mechanism of crystal growth change with the addition of Sb to the binary $Se_{90}M_{10}$ (M=In, Zn) composition. For glasses ternary $Se_{90-x}In_{10}Sb_x$ (x = 2, 4) and $Se_{90-x}Zn_{10}Sb_x$ (x= 2, 4) compositions, the values of n = 4 and m = 3 suggested the bulk nucleation with three dimensional growth. For glasses binary $Se_{90}In_{10}$ and $Se_{90}Zn_{10}$ compositions, the values of n=3 and m=2 suggested the bulk nucleation with two-dimensional growth.

Table 4: The Values of Avrami index *n* and dimensionality of growth *m* for the composition $Se_{90-x}In_{10}Sb_x$ (x = 0, 2, 4) glassy alloys.

	X= In								
Sample	$Se_{90}In_{10}$			$Se_{88}In_{10}Sb_2$			$Se_{86}In_{10}Sb_4$		
T (K)	409	413	421	403	409	413	399	403	407
n	3.17 ±0.09	3.24 ±0.19	2.98 ±0.08	4.45 ±0.19	4.02 ±0.16	3.71 ±0.13	4.31 ±0.20	4.42 ±0.23	4.19 ±0.22
Average value *n*	3.13 ± 0.12			4.06 ± 0.16			4.30 ± 0.22		
m	2			3			3		

Table 5: The Values of Avrami index *n* and dimensionality of growth *mm* for the composition $Se_{90-x}Zn_{10}Sb_x$ (x = 0, 2, 4) glassy alloys.

	X=Zn								
Sample	$Se_{90}Zn_{10}$			$Se_{88}Zn_{10}Sb_2$			$Se_{86}Zn_{10}Sb_4$		
T (K)	384	392	400	405	411	415	402	407	415
n	4.14 ±0.52	3.21 ±0.10	2.13 ±0.18	4.49 ±0.15	3.85 ±0.26	4.03 ±0.25	4.39 ±0.22	4.26 ±0.28	3.66 ±0.40
Average value *n*	3.16 ± 0.26			4.12 ±0.22			4.10 ± 0.30		
m	2			3			3		

The plots of ln[-ln(1-*x*)] versus 1000/T for the composition $Se_{88}In_{10}Sb_2$ and $Se_{88}Zn_{10}Sb_2$ at different heating rates are shown in Figure 6. From the slopes of the straight lines, the average values of E_c for different compositions were calculated and listed in Table 6.
It is observed from Fig. 10.11 that, the plots are linear over a wide temperature rang. At higher temperatures a break is seen in the linearity for all heating rates. This break may be considered due to the saturation of the nucleation sites at the final stage of crystallization [34] or to the restriction of crystal growth by the small size of the particles [35].

3.2.2 Kissinger method
The Kissinger model [26] has been established, also, in dynamical regime. As opposite to the model of Matusita, it is considered that on the top of crystallization peak the amount of crystallized fraction is x=0.63. The Kissinger equation has the form.

$$\ln\left(\alpha / T_p^{\,2}\right) = -E_c / RT_p + \text{constant} \qquad (6)$$

Where T_p is the temperature corresponding to the top of the crystallization peak.

The Plots of Ln (α/T_p^2) vs 1000/ T_p for glasses $Se_{90-x}In_{10}Sb_x$ (x= 0, 2, 4) and $Se_{90-x}Zn_{10}Sb_x$ (x= 0, 2, 4) compositions are shown in Figure 7. The data are fitted by straight lines. The slope of the straight line gives the activation energy of crystallization. The estimated values of Ec for the studied compositions are listed in Table 7.

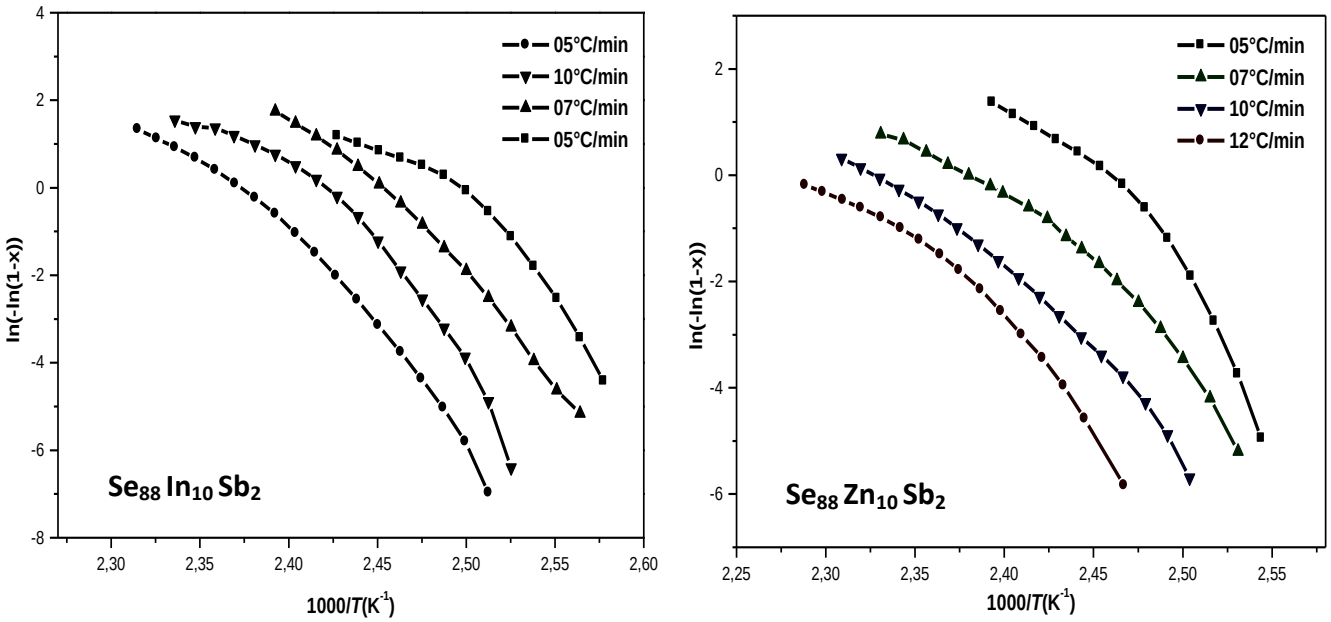

Figure 6: the plots of ln[-ln(1-x)] versus 1000/T at different heating rates for $Se_{88}In_{10}Sb_2$ and $Se_{88}Zn_{10}Sb_2$glasses

Table 6: The values of activation energy of crystallisation obtained from Matusita method

	Composition	E_c / KJ.mol^{-1}	E_c / eV
X=In	$Se_{90}In_{10}$	106.39 ± 3.54	1.10 ± 0.03
	$Se_{88}In_{10}Sb_2$	92.17 ± 5.52	0.95 ± 0.05
	$Se_{86}In_{10}Sb_4$	86.90 ± 4.87	0.90 ± 0.05
X=Zn	$Se_{90}Zn_{10}$	93.53 ± 8.42	0.96 ± 0.08
	$Se_{88}Zn_{10}Sb_2$	104.44 ± 6.60	1.08 ± 0.06
	$Se_{86}Zn_{10}Sb_4$	127.52 ± 4.30	1.32 ± 0.04

3.2.3 Ozawa method

The activation energy of crystallization can also be calculated from the variation in the onset crystallization temperature T_c with heating rate using the Ozawa equation [36]:

$$\ln \alpha = -E_c / RT_p + \text{constant} \quad . \qquad (7)$$

Figure 8 shows the variation of Lnα against 1000/ T_p for the studied compositions $Se_{90-x}In_{10}Sb_x$ (x= 0, 2, 4) and $Se_{90-x}Zn_{10}Sb_x$ (x= 0, 2, 4) glasses. E_c can be calculated from the slope of the obtained straight lines. The deduced values of E_c for the studied compositions are listed in Table 7.

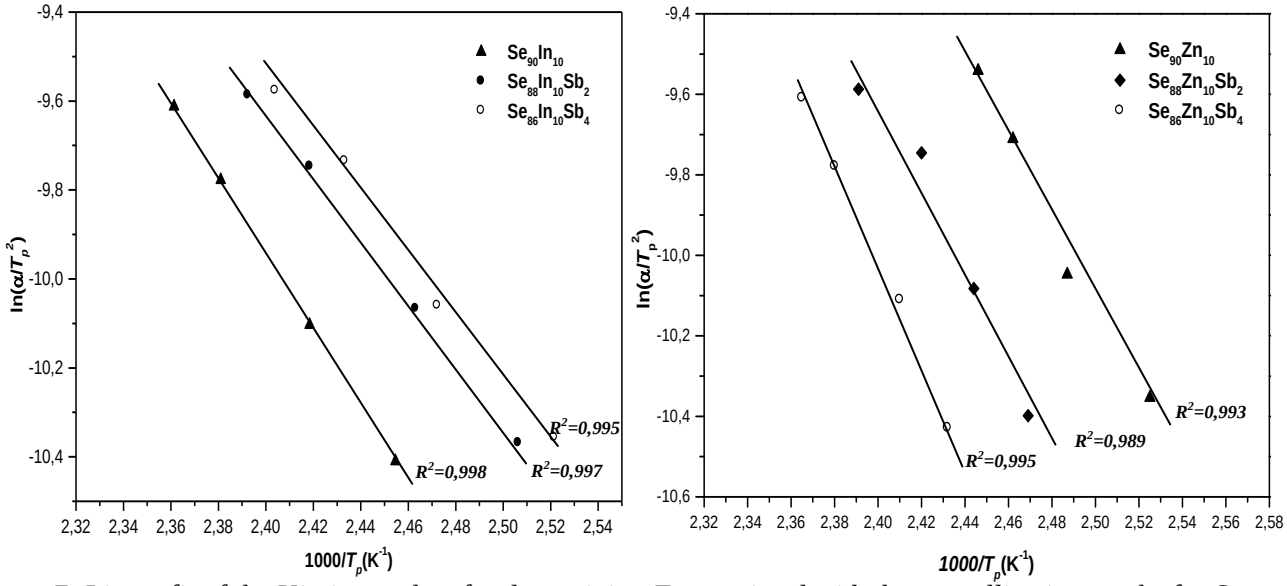

Figure 7: Linear fit of the Kissinger plots for determining E_c associated with the crystallization peaks for $Se_{90-x}In_{10}Sb_x$ and $Se_{90-x}Zn_{10}Sb_x$ (x=0, 2, 4) glasses.

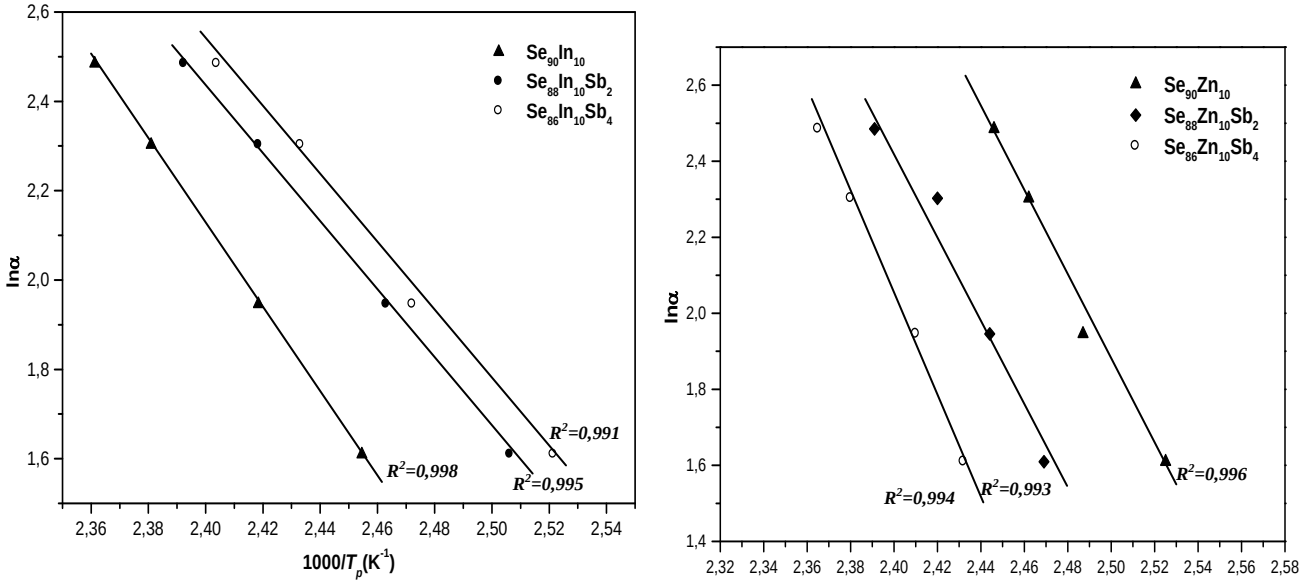

Figure 8: Linear fit of the Kissinger plots for determining E_c associated with the crystallization peaks for $Se_{90-x}In_{10}Sb_x$ and $Se_{90-x}Zn_{10}Sb_x$ (x=0, 2, 4) glasses.

Table 7: The values of activation energy of crystallisation obtained from Kissinger and Ozawa methods.

		Kissinger		Ozawa	
	Composition	E_c / KJ.mol^{-1}	E_c / eV	E_c / KJ.mol^{-1}	E_c / eV
X=In	$Se_{90}In_{10}$	68.24 ± 0.25	0,71 ± 0.01	75.14 ± 0.30	0,78 ± 0.01
	$Se_{88}In_{10}Sb_2$	52.03 ± 0.91	0,54 ± 0.01	58.85 ± 0.91	0,61 ± 0.01
	$Se_{86}In_{10}Sb_4$	51.12 ± 2.90	0,53 ± 0.03	57.85 ± 2.90	0,60 ± 0.03
X=Zn	$Se_{90}Zn_{10}$	85.86 ± 7.06	0.89 ± 0.07	92.50 ± 8.39	0.95 ± 0.08
	$Se_{88}Zn_{10}Sb_2$	89.84 ± 8.56	0.93 ± 0.08	96.74 ± 12.38	1.00 ± 0.12
	$Se_{86}Zn_{10}Sb_4$	98.49 ± 6.17	1.02 ± 0.06	105.39 ± 3.90	1.09 ± 0.04

It is observed from Table 7 that values of activation energy of crystallization E_c obtained from all three models Matusita model, Kissinger model, and Ozawa model increases with the increase in antimony (Sb) for $Se_{90-x}Zn_{10}Sb_x$ glassy alloys but for the composition $Se_{90-x}In_{10}Sb_x$ the activation energy of crystallization decreases with the increase in Sb. The addition of antimony has one side change mechanisms of nucleation and growth, and on the other side braked crystallization as in the case M = Zn or the crystallization is accelerated in the case M = In.

The values of activation energy of crystallization E_c for $Se_{90-x}In_{10}Sb_x$ and $Se_{90-x}Zn_{10}Sb_x$ (x=0, 2, 4 compositions determined according to Kissinger and Ozawa methods are in good agreement with each other but different from its value obtained according to the Matusita method. This difference may be due to the different approximations used in this method.

3.3. Thermal stability

In non-isothermal study, the temperature difference between the onset temperature of crystallization T_c and the glass transition temperature T_g is important indicator of the thermal stability [37]. the higher the value of this difference, the more the delay in the nucleation process.

Figure 9 shows the variation of $T_c - T_g$ with percentage composition of Sb in the $Se_{90-x}M_{10}Sb_x$ (M= In, Zn) x= (0, 2, 4) glasses. It is also noted from fig. 14 that the thermal stability is at a maximum when the Sb content reaches 4 at. % for $Se_{90-x}Zn_{10}Sb_x$ and highest for $Se_{90}In_{10}$.

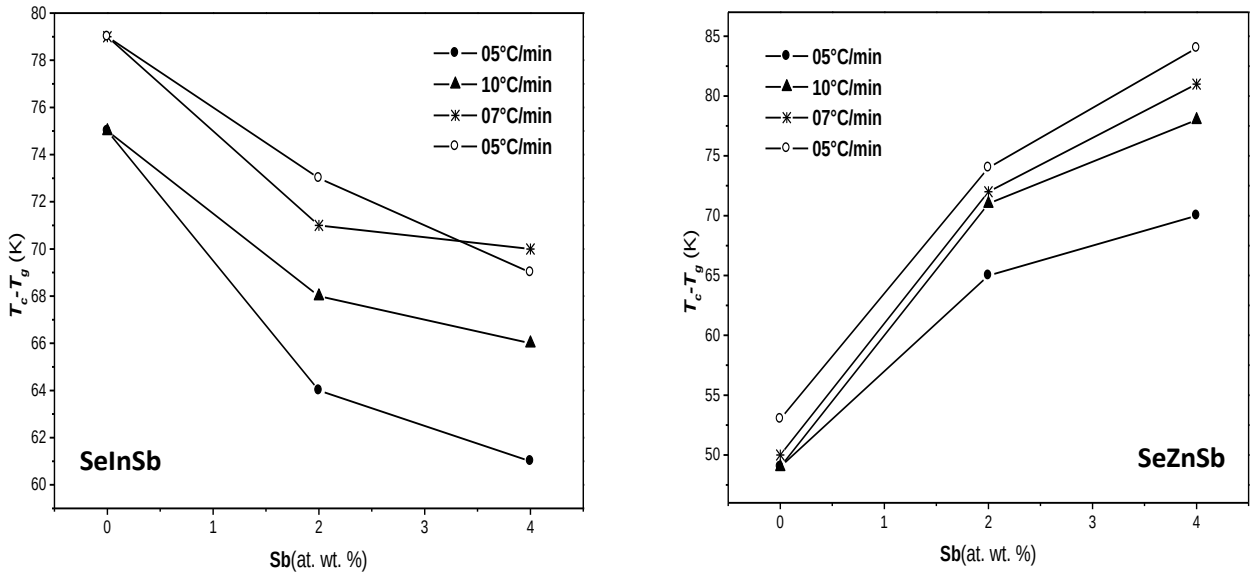

Figure 9: Variation of $T_c - T_g$ with atomic weight percentage of Sb.

Conclusion

The kinetics of glass transition and crystallization in glasses $Se_{90-x}M_{10}Sb_x$ (M= In, Zn) alloys have been studied by non-isothermal DSC technique.

The results show that all compositions have a single glass transition and single stage crystallization. The observed dependence of T_g on heating rates was used to evaluate E_g.

The activation energies of the glass transition and crystallization processes for these chalcogenide glasses have been calculated using the different non-isothermal methods. The calculated values of the kinetic exponent n suggest two dimensional growth for the binary $Se_{90}M_{10}$ (M=In, Zn) and three dimensional growth for ternaries $Se_{90-x}In_{10}Sb_x$ (x = 2, 4), $Se_{90-x}Zn_{10}Sb_x$ (x= 2, 4).

The addition of antimony has one side change mechanisms of nucleation and growth, and on the other side braked crystallization as in the case M = Zn or the crystallization is accelerated in the case M = In.

References

1. Sanghera J., Shaw L. B., Busse L., Nguyen V., Pureza P., Cole B., Harbison B.B., Aggarwal I., *Fiber and Integrated Optics*. 19 (2000) 251.
2. Yamada N., Ohno E., Akahira N., Nishiuchi K., Nagata K., Takao M., *Japan J. Appl. Phys*. 26 (1987).
3. Thornburg D., *J. Non Cryst. Solids*. 2 (1972) 131.
4. Hunt D. C., Kirby S.S., Rowlands, J. A., *Med. Phys*. 29 (2002) 2464.
5. Zhang J., Zhang S.Y., Xu J.J., Chen H.Y., *Chinese Chem Lett*. 15 (2004) 1345.
6. Le Neindre L., Smektala F., Le Foulgoc K., Zhang X.H., Lukas J., *J. Non-Cryst. Solids*. 24 (1989) 299.
7. Akiyama T., Uno M., Kitaura H., Narumi K., Kojima R., Nishiuchi K., Yamada N., *Jpn. J. Appl Phys*. 40 (2001) 1598.
8. Ohta T., *J. Optoelectron. Adv. Mater*. 3 (2001) 609.
9. Heireche M.M., Belhadji M., Hakiki N.E., *J. Therm. Anal. Calorim*. 114 (2013) 195.
10. Heireche L., Heireche M.M., Belhadji M., *J. Cryst. Process Technol*. 4 (2014) 111.
11. Abdel-Rahim M.A., Hafiz M.M., Abdel-Latief A.Y., Abd-Elnaiem A.M., Elwhab A., Alwany B., *Appl. Phys. A*. 119 (2015) 881.
12. Shaaban, E.R., Elshaikh A., Soraya M.M., *Int. J. New. Hor. Phys*. 1 (2014) 9.
13. Su X., Wang R., Luther-Davies B., Wang Li., *Appl. Phys*. 113 (2013) 575.
14. Chander R., Thangaraj R., *Appl. Phys. A*. 99 (2010) 181.
15. Fouad S.S., El-Bana M.S., Sharma P., Sharma V., *Appl. Phys. A*. 120 (2015) 137.
16. Farid A.S., Atyia H.E., *J. Non-Cryst Solids*. 408 (2015) 123.
17. Aly A., Afify N., Abousehlly A.M., Abd Elnaeim A., M., *J. Non-Cryst. Solids*. 357 (2011) 2029.
18. Sharma P., Katyal S.C., *J. Non-Cryst. Solids*. 354 (2008) 3836.
19. Sharma P., Dahshan A., Aly K. A., *Dalton Transactions*. 44 (2015) 14799.
20. Sharma N., Patial1 B.S., Thakur N., *Applied Physics A*. 122 (2016) 209.
21. Mehta N., Singh K., Saxena N.S., *Solid state sciences*. 12 (2010) 963.
22. Segura A., Guesdon J.P., Besson J.M., Suzuki A., *J. Appl. Phys*. 54 (1983) 876.
23. Bhargava R.N., *IEE INSPEC (London, U.K.)*. 17 (1997) 134.
24. Lasocka M., *Mater Sci Eng*. 23 (1976) 173.
25. Faheem Naqvi S., Saxena N.S., *J. Therm Anal Calorim*. 108, (2012) 1161.
26. Kissinger H.E., *Anal Chem*., 29, (1957) 1702.
27. Avrami M., *J. Chem Phys*. 7, (1939) 1103.
28. Avrami M., *J. Chem Phys*. 8, (1940) 212.
29. Avrami M., *J. Chem Phys*. 9, (1941) 177.
30. Afify N., *J.Non-Cryst.Solids*. 142, (1992) 247.
31. Matusita K., Konastsu T.,Yokota R., *J. Materials Science*. 19, (1984) 291.
32. Ziani N., Belhadji M., Heireche L., Bouchaour Z., Belbachir M., *Physica B: Condensed Matter*. 358 (2005) 132.
33. Mahadevan S., Giridhar A., Singh A.K., *J. Non-Cryst. Solids*. 88 (1986) 11.
34. Colmenero J., Barandiaran J.M., *J. Non-Cryst. Solids*. 30 (1979) 263.
35. Kaur G., Komatsu T., *J. Mater Sci*. 36 (2001) 4531.
36. Ozawa T., *Bulletin of the Chemical Society of Japan*. 38 (1965) 1881.
37. Hruby A., *Czechoslov J Phys B*. 22 (1972) 1187.